Anomalous Fermi's golden rule and transition dynamics at non-Hermitian exceptional points

Yifei Yi(易益妃)[1]

[1] *Sichuan Normal University, Chengdu, Sichuan 610066, China*

(Dated: 2026 年 10 月 8 日)

Fermi' s golden rule (FGR), whose origins date back to the early days of quantum mechanics, has recently been extended to non-Hermitian systems. However, generalizations of FGR to non-Hermitian systems have largely been built upon the biorthogonal basis formalism, which presupposes the diagonalizability of the Hamiltonian. The problem becomes much more complicated when the Hamiltonian possesses exceptional points (EPs), where the eigenvectors coalesce and the Hamiltonian becomes defective (non-diagonalizable). In this work, by computing the evolution of the associated Jordan block in the interaction picture, we derived FGR for systems containing an EP of order 2. We found that in the short-time limit, the transition probability P exhibits an anomalous t^4 scaling, rather than $P \propto t^2$ as in non-Hermitian systems without EPs. On the other hand, in the long-time limit, the system exhibits a Squared-Lorentzian resonance lineshape that is sharper than the conventional Lorentzian profile observed in a non-Hermitian system without EPs. Numerical simulations verify the analytical results.

Keywords: Non-Hermitian systems, Exceptional points, Fermi' s golden rule

PACS: 03.65.Aa, 03.65.Yz

I. INTRODUCTION

Linear response theory (LRT) and the associated Fermi's golden rule (FGR) constitute the rigorous mathematical foundation for describing the macroscopic response and microscopic quantum transitions of physical systems subjected to weak external perturbations [1–7]. This formalism has been extensively used in standard quantum mechanics to study both linear and nonlinear dynamical behaviors, and now it begins to be extended to non-conservative systems [8–12].

In standard quantum mechanics, the Hamiltonian is assumed to be Hermitian. However, nonequilibrium and open systems are effectively described by non-Hermitian Hamiltonians. In recent years, research on non-Hermitian physics has progressed remarkably in both experiments and theory [13–22]. Benefiting from the development of synthetic dimensions and precise quantum control, non-Hermitian Hamiltonians have been successfully realized across diverse physical platforms, including classical photonics [23–25], open quantum systems [26–28], and cold atoms [29, 30]. At the heart of this fast-growing field lies a key goal: extending the basic principles of standard quantum mechanics to the non-Hermitian realm.

To date, generalizations of LRT and FGR to non-Hermitian systems have been achieved primarily by employing the biorthogonal basis [31]. However, these existing frameworks inherently rely on the assumption of diagonalizability of the Hamiltonian, and this assumption breaks down at non-Hermitian exceptional points (EPs) [32–40], where not only the eigenvalues but also the corresponding eigenstates coalesce. Although recent studies on non-Hermitian sensors have revealed that the steady-state response at an EP under continuous-wave driving exhibits a squared-Lorentzian profile, the microscopic, time-domain transition dynamics driven by a time-dependent perturbation exactly at an EP remains a open question.

In this work, we derive an anomalous FGR for defective non-Hermitian systems that possesses an exceptional point of order 2 (EP2). By formulating the time-dependent perturbation theory within the interaction picture, we unveil the unique quantum transition dynamics at an EP2. We demonstrate that in contrast to the conventional FGR predicting a short-time transition probability scaling as $P \propto t^2$, the coalesced system exhibits an anomalous $P \propto t^4$ scaling in the short-time limit. Furthermore, it is also found that the system exhibits exotic dynamical response in the long-time limit, that is, a steady-state squared-Lorentzian resonance profile, as opposed to the ordinary Lorentzian lineshape observed in non-Hermitian systems without EPs. Our analytical predictions are verified by exact numerical simulations. This theoretical framework repairs the breakdown of standard perturbation theory at EPs, and provides a microscopic time-domain perspective for understanding transient signal transduction at non-Hermitian degeneracies, which may inspire novel dynamic schemes for weak-signal detection.

II. MODEL AND BREAKDOWN OF CONVENTIONAL FGR

In this work, we study a three-level system containing an EP of order 2, whose Hamiltonian, in its mathematically simplest form (the Jordan canonical form), is given by (we use natural units $\hbar = 1$ throughout):

$$\hat{H}_0 = \begin{pmatrix} E_1 & 0 & 0 \\ 0 & E_{ep} & J \\ 0 & 0 & E_{ep} \end{pmatrix} \tag{1}$$

The basis $\{|1\rangle, |2\rangle, |3\rangle\}$ employed here has the following properties: $|1\rangle$ is a Hermitian eigenstate, i.e., its eigenvalue E_1 is real and it is orthogonal to both $|2\rangle$ and $|3\rangle$; $|2\rangle$ is an eigenstate with a generally complex eigenvalue denoted $E_{ep} = \epsilon - i\gamma$ ($\epsilon, \gamma \in \mathbb{R}$), where ϵ is the resonance energy, and $\gamma > 0$ is the dissipation rate; $|3\rangle$ is a generalized eigenstate satisfying $(\hat{H}_0 - E_{ep})|3\rangle = J|2\rangle \neq 0$.

In this basis, both the unperturbed time-evolution operator $\hat{U}_0(t) = e^{-i\hat{H}_0 t}$ and its inverse $\hat{U}_0^{-1}(t) = e^{i\hat{H}_0 t}$ can be written as upper triangular matrices:

$$\hat{U}_0(t) = \begin{pmatrix} e^{-iE_1 t} & 0 & 0 \\ 0 & e^{-iE_{ep}t} & -iJte^{-iE_{ep}t} \\ 0 & 0 & e^{-iE_{ep}t} \end{pmatrix}, \tag{2}$$

and

$$\hat{U}_0^{-1}(t) = \begin{pmatrix} e^{iE_1 t} & 0 & 0 \\ 0 & e^{iE_{ep}t} & iJte^{iE_{ep}t} \\ 0 & 0 & e^{iE_{ep}t} \end{pmatrix}. \tag{3}$$

Note that the time evolution within the excited-state subspace acquires an algebraically growing term proportional to t (specifically, the off-diagonal element $-iJt$), in stark contrast to the purely exponential behavior found in Hermitian systems as well as in non-Hermitian systems without EPs.

Now we add a harmonic perturbation $\hat{V}(t) = \hat{V}e^{i\omega t}$ at time $t = 0$, where

$$\hat{V} = \begin{pmatrix} 0 & 0 & 0 \\ V_{21} & 0 & 0 \\ V_{31} & 0 & 0 \end{pmatrix} \tag{4}$$

In Hermitian systems, or non-Hermitian systems without EPs, the (right) eigenstates $\{|\phi_n\rangle\}$ of the Hamiltonian form a complete set in the Hilbert space. Consequently, for an arbitrary initial state $|\psi_0\rangle$, we can expand it as $|\psi_0\rangle = \sum_n c_n |\phi_n\rangle$. Assuming that the state evolves into $|\psi(t)\rangle = \sum_n c_n(t)e^{-iE_n t}|\phi_n\rangle$ at an arbitrary time t, the expansion coefficients $c_i(t)$ can be calculated using the projection $\langle\phi_i|\psi(t)\rangle$, or the biorthogonal projection $\langle\chi_i|\psi(t)\rangle$ for non-Hermitian systems, where $|\chi_i\rangle$ is one of the left eigenvector of the Hamiltonian. However, for the case where the spectrum of the Hamiltonian contains an EP of order 2, i.e., formed by the coalescence of two eigenstates. the eigenstates do not form a complete basis. Since the Hamiltonian is defective, the state cannot be expressed using the aforementioned simple expansion.

In the following, we rederive FGR for non-Hermitian systems with EP2 within the interaction picture. In the Schrödinger picture, the state vector contains all the dynamical information and is simultaneously affected by the intrinsic evolution of the system and by the perturbation, making it difficult to disentangle their respective contributions. By contrast, the interaction picture isolates the transition dynamics from the non-Hermitian background evolution, thereby clarifying the physical picture of "transition" and making the first-order perturbation approximation mathematically straightforward and natural. It is also worth noting that while the exact dynamics can be directly solved in the Schrödinger picture (as we will employ later for numerical verification), the interaction picture analytically unveils how the Jordan block directly modifies the effective perturbation Hamiltonian with an algebraic time-dependence.

III. FIRST-ORDER PERTURBATION EXPANSION IN THE INTERACTION PICTURE

We start from the Schrödinger equation. The total Hamiltonian of the system is $\hat{H}(t) = \hat{H}_0 + \hat{V}(t)$, and the state vector satisfies the following time-dependent Schrödinger equation:

$$i\frac{\partial}{\partial t}\left|\Psi(t)\right\rangle = \left[\hat{H}_0 + \hat{V}(t)\right]\left|\Psi(t)\right\rangle. \tag{5}$$

To treat the time-dependent perturbation, we transform to the interaction picture. The state vector in the interaction picture, denoted by $|\Psi_I(t)\rangle$, is defined as

$$\left|\Psi_I(t)\right\rangle = \hat{U}_0^{-1}(t)\left|\Psi(t)\right\rangle. \tag{6}$$

We expand the state vectors in two pictures as $|\Psi(t)\rangle = \{C_1(t), C_2(t), C_3(t)\}^T$, and $|\Psi_I(t)\rangle = \{c_1(t), c_2(t), c_3(t)\}^T$, respectively. Then we readily obtain:

$$\begin{pmatrix} c_1(t) \\ c_2(t) \\ c_3(t) \end{pmatrix} = \begin{pmatrix} C_1(t)e^{iE_1 t} \\ [C_2(t) + iJtC_3(t)]e^{iE_{ep}t} \\ C_3(t)e^{iE_{ep}t} \end{pmatrix}, \tag{7}$$

or

$$\begin{pmatrix} C_1(t) \\ C_2(t) \\ C_3(t) \end{pmatrix} = \begin{pmatrix} c_1(t)e^{-iE_1 t} \\ [c_2(t) - iJtc_3(t)]e^{-iE_{ep}t} \\ c_3(t)e^{-iE_{ep}t} \end{pmatrix}. \tag{8}$$

Combining Eq. (5) with Eq. (6) yields the evolution equation for the interaction picture state:

$$i\frac{\partial}{\partial t}\left|\Psi_I(t)\right\rangle = \hat{V}_I(t)\left|\Psi_I(t)\right\rangle, \tag{9}$$

with $\hat{V}_I(t) = \hat{U}_0^{-1}(t)\hat{V}(t)\hat{U}_0(t)$ being the perturbation operator in the interaction picture. The above equation can be further computed as follows:

$$\begin{aligned} i\frac{\partial}{\partial t}\begin{pmatrix} c_1(t) \\ c_2(t) \\ c_3(t) \end{pmatrix} &= \hat{U}_0^{-1}(t)\hat{V}(t)\hat{U}_0(t)\begin{pmatrix} c_1(t) \\ c_2(t) \\ c_3(t) \end{pmatrix} \\ &= \begin{pmatrix} 0 & 0 & 0 \\ (V_{21} + iJtV_{31})e^{izt} & 0 & 0 \\ V_{31}e^{izt} & 0 & 0 \end{pmatrix}\begin{pmatrix} c_1(t) \\ c_2(t) \\ c_3(t) \end{pmatrix} \\ &= \begin{pmatrix} 0 \\ (V_{21} + iJtV_{31})e^{izt}c_1(t) \\ V_{31}e^{izt}c_1(t) \end{pmatrix}, \end{aligned} \tag{10}$$

where $z = E_{ep} - E_1 - \omega$ is the complex detuning, or it can be explicitly written as $z = \Delta - i\gamma$, with $\Delta = \epsilon - E_1 - \omega$ being the real detuning.

We assume that the system is entirely in the ground state $|1\rangle$ at $t = 0$, i.e., $c_1(0) = 1, c_2(0) = c_3(0) = 0$. If we confine our discussion to the case of weak perturbation and assume that the coefficients do not change much during time t, then, as a first-order approximation, we can substitute $c_1(t) \approx c_1(0) = 1$ into the above equation, which gives the decoupled differential equations satisfied by $c_2(t)$ and $c_3(t)$:

$$i\dot{c}_3(t) = V_{31}e^{izt}. \tag{11}$$

$$i\dot{c}_2(t) = (V_{21} + iJtV_{31})e^{izt}. \tag{12}$$

Integrating the above equations yields

$$c_3(t) = -iV_{31}\int_0^t e^{iz\tau}d\tau = V_{31}\frac{1 - e^{izt}}{z}, \tag{13}$$

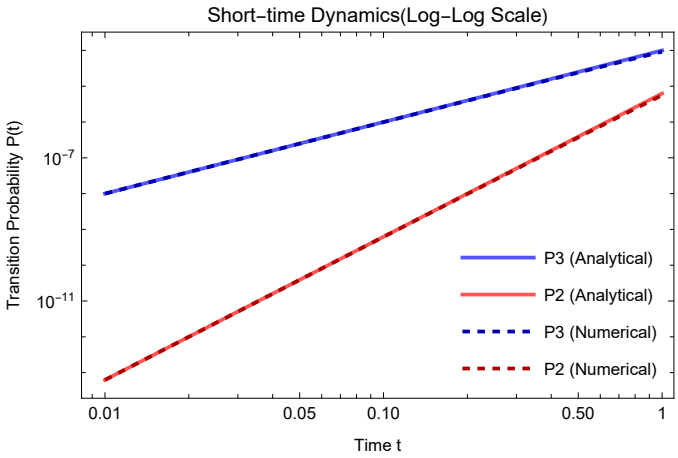


图 1. Log-log plot of short-time dynamics. The blue and red solid lines are obtained from the analytical expressions, Eqs. (17) and (18), respectively, while the dark blue and dark red dashed lines are from direct numerical solutions of the Schrödinger equation Eq. (5). The parameters are set to be: $E_1 = 0.2$, $\epsilon = 1$, $\gamma = 0.08$, $J = 0.5$, $\omega = 1$, $V_{21} = 0$, $V_{31} = 0.01$.

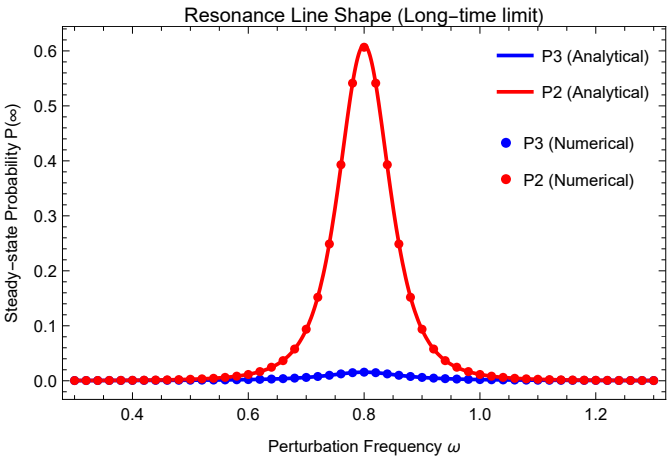


图 2. Steady-state resonance lineshape. The blue and red solid lines are obtained from the analytical expressions, Eqs. (20) and (21), respectively, while the dark blue and dark red dashed lines are from direct numerical solutions of the Schrödinger equation Eq. (5). The blue curve corresponds to the Lorentzian lineshape, while the red curve corresponds to the squared-Lorentzian lineshape. The parameters are set to be: $E_1 = 0.2$, $\epsilon = 1$, $\gamma = 0.08$, $J = 0.5$, $V_{21} = 0$, $V_{31} = 0.01$, $t = 100$.

and

$$c_2(t) = -i\int_0^t (V_{21} + iJ\tau V_{31})e^{iz\tau}d\tau = \frac{V_{21}z - JV_{31}}{z^2}(1 - e^{izt}) - i\frac{JV_{31}t}{z}e^{izt}. \quad (14)$$

The above result is obtained within the interaction picture. However, it should be noted that in non-Hermitian systems, "transition" and "dissipation" represent two competing physical processes, which are both physically genuine and indispensable. The interaction picture exclusively accounts for pure transitions, whereas the Schrödinger picture yields the realistic observational outcomes that incorporate the intrinsic background dissipation. Thus, tn order to correspond to the physical observables measured in realistic non-Hermitian experiments, it is necessary to transform back to the Schrödinger picture.

Substituting Eqs. (13) and (14) into Eq. (8), we have

$$C_3(t) = V_{31}\frac{e^{-iE_{ep}t} - e^{-i(E_1+\omega)t}}{z}, \quad (15)$$

and

$$C_2(t) = \frac{V_{21}z - JV_{31}}{z^2}[e^{-iE_{ep}t} - e^{-i(E_1+\omega)t}] - i\frac{JV_{31}t}{z}e^{-iE_{ep}t}. \quad (16)$$

This is the analytical result obtained under the first-order perturbation approximation. In what follows, we separately discuss the response behaviors in the short-time and long-time limits.

A. Short-time Anomalous Dynamics

To investigate the short-time dynamics, we perform a Taylor expansion on the terms $e^{-iE_{ep}t}$ and $e^{-i(E_1+\omega)t}$ in the limit $t \to 0$, respectively: $e^{-iE_{ep}t} \approx 1 - iE_{ep}t - E_{ep}^2t^2/2$ and $e^{-i(E_1+\omega)t} \approx 1 - i(E_1+\omega)t - (E_1+\omega)^2t^2/2$. Substituting the expansions into Eq. (15) and Eq. (16), and retaining only the leading-order term, we obtain, respectively,

$$P_3(t \to 0) = |C_3(t \to 0)|^2 \approx |V_{31}|^2t^2, \quad (17)$$

i.e., $P_3 \propto t^2$, which is in agreement with the behavior observed in Hermitian systems and in non-Hermitian systems far from the EPs (see Appendix A and Appendix B for details), and,

$$P_2(t \to 0) = |C_2(t \to 0)|^2 \approx \frac{1}{4}|J|^2|V_{31}|^2 t^4, \qquad (18)$$

exhibiting an anomalous t^4 scaling law. In the above calculation, the parameter V_{21} is set to be zero.

As we have previously pointed out, state $|3\rangle$ is a generalized eigenstate that satisfies $H_0|3\rangle = E_{ep}|3\rangle + J|2\rangle$, which implies that, owing to the presence of the off-diagonal coupling term J, the probability amplitude of state $|3\rangle$ will spontaneously flow into state $|2\rangle$. Setting $V_{21} = 0$ effectively forbids any direct transition from state $|1\rangle$ to state $|2\rangle$. Thus, state $|2\rangle$ can only be pumped through a coherent two-step cascade:

$$|1\rangle \xrightarrow{V_{31}} |3\rangle \xrightarrow{J} |2\rangle \qquad (19)$$

In this way, the anomalous response can be prevented from being masked by the ordinary background, thus enabling the detection of the response specific to the EP system. From an experimental perspective, the condition $V_{21} = 0$ can be realized by symmetry selection rules or spatial mode matching in realistic platforms. For instance, in atomic or molecular non-Hermitian systems, this selective excitation can be strictly enforced by optical dipole selection rules. If state $|1\rangle$ shares the same parity as state $|2\rangle$, which is opposite to that of state $|3\rangle$, then the direct transition from state $|1\rangle$ to state $|2\rangle$ is intrinsically forbidden. Furthermore, in macroscopic platforms such as coupled whispering-gallery-mode microcavities or superconducting microwave circuits, $V_{21} = 0$ naturally arises from the spatial arrangement of the setup. By placing the external driving waveguide (state $|1\rangle$) such that it couples solely to the first cavity (state $|3\rangle$), the direct excitation to the remote second cavity (state $|2\rangle$) is physically blocked, i.e., $V_{21} = 0$.

Eq. (18) indicates that the coalescence of eigenstates gives rise to exotic dynamics, i.e., $P_2 \propto t^4$ instead of $P_2 \propto t^2$, in the short-time transition probability.

Fig.1 presents a comparison between the results obtained by direct numerical solution of the Schrödinger equation, i.e., Eq. (5) and those derived from the analytical expressions in Eqs. (17) and (18). To illustrate the short-time dynamical behavior, the time t is confined to the interval $[0, 5]$. The two sets of results are found to be in good agreement.

B. Steady-state Anomalous Resonance Profile

We now turn to the steady-state response ($t \to \infty$). Owing to the presence of factor $e^{-\gamma t}$ (noting that $\gamma > 0$, i.e., dissipation is present), the term $e^{-iE_{ep}t}$ in Eqs. (15) and (16) vanishes at $t \to \infty$. Accordingly, the steady-state behavior can be derived:

$$P_3(\infty) = |C_3(\infty)|^2 = \frac{|V_{31}|^2}{|z|^2} = \frac{|V_{31}|^2}{\Delta^2 + \gamma^2}, \qquad (20)$$

and (V_{21} is also set to 0),

$$P_2(\infty) = |C_2(\infty)|^2 = \frac{|J|^2|V_{31}|^2}{|z|^4} = \frac{|J|^2|V_{31}|^2}{(\Delta^2 + \gamma^2)^2}, \qquad (21)$$

As a function of the driving frequency ω, Eq. (20) exhibits a conventional Lorentzian resonance peak that centered at $\omega = \epsilon - E_1$, with a full width at half maximum equal to 2γ. This steady-state response is identical to that observed in non-Hermitian systems without EPs (see Appendix B for details).

Eq. (21), on the other hand, manifests a squared-Lorentzian lineshape, which indicates that in the presence of EPs, the absorption spectrum exhibits sharper resonant features, as shown in Fig.2.

Fig.2 presents a comparison between the results obtained by direct numerical solution of the Schrödinger equation, i.e., Eq. (5) and those derived from the analytical expressions in Eqs. (20) and (21). We can see that the two sets of results are in good agreement.

We finally note that, recently, it has been demonstrated in non-Hermitian photonics and sensors that the steady-state transmission spectrum at an EP

of order M can exhibit a Lorentzian response or a super-Lorentzian response of order M_s, with $M_s = 2, 3, \ldots, M$, see, for example, Ref. [9], which investigated the steady-state/frequency-domain response of driven EP systems. Meanwhile, our present work in fact explores the microscopic time-domain mechanism at an EP by developing FGR applicable to the defective Hamiltonian, and fills the theoretical gap resulting from the breakdown of the biorthogonal-basis-based FGR.

IV. CONCLUSIONS AND DISCUSSIONS

In this work, we derive FGR for the non-Hermitian systems with an EP of order 2. In order to isolate the transition dynamics from the non-Hermitian background evolution, the majority of our calculations is carried out in the interaction picture. For consistency with experimental results, we eventually revert to the Schrödinger picture and present the analytical solution within the first-order perturbation approximation. We have separately discussed the responses in the short-time limit and those in the long-time limit (the steady-state response), and found that in the short-time limit, the transition probability exhibits an anomalous t^4 scaling. And in the long-time limit, the system exhibits a Squared-Lorentzian resonance lineshape.

Our theory can be experimentally validated by mapping the abstract three-level model onto a realistic physical platform: two coupled optical whispering-gallery-mode microcavities or superconducting microwave resonators. Consider two coupled resonators (denoted as mode a and mode b) with identical resonant frequency ω_0 but asymmetric decay rates γ_a and γ_b. The effective non-Hermitian Hamiltonian is given by

$$H_{cav} = \begin{pmatrix} \omega_0 - i\gamma_a & \kappa \\ \kappa & \omega_0 - i\gamma_b \end{pmatrix} \tag{22}$$

where κ is the inter-cavity coupling strength. By tuning the system parameters to satisfy $\kappa = |\gamma_1 - \gamma_2|/2$, the system coalesces into a EP2. In this context, the initial state $|1\rangle$ in our model corresponds to the external continuous-wave driving field acting as the unperturbed source, and a weak incoming signal acts as the time-dependent perturbation $V(t)$ that predominantly couples into one of the cavities. Such highly controllable microcavity platforms have already been widely used in steady-state EP sensing, making our time-domain theoretical predictions highly accessible for experimental verification.

It should be noted that, while the ultimate sensitivity limit in practical sensors strictly depends on the signal-to-noise ratio involving complex noise dynamics, this t^4 algebraic growth that appears in our anomalous FGR provides a novel transient temporal window that could be potentially exploited to rapidly outpace static technical noises during the initial detection stage.

Finally, for an EP of order N, the corresponding Jordan block introduces higher-order polynomial terms (up to t^{N-1}) in the time-evolution operator. It is thus physically expected that a sequential cascade transition through these higher-order generalized eigenstates could lead to an even steeper transient algebraic scaling. However, rigorously formulating the transition dynamics for arbitrary N-th order EPs remains an open question for future investigations.

V. ACKNOWLEDGEMENT

This work was supported by the National Natural Science Foundation of China (Grant No.12304201).

[1] Dirac P A M 1927 *Proc. R. Soc. A* **114** 243–265

[2] Fermi E 1932 *Rev. Mod. Phys.* **4** 87–132

[3] Kubo R 1957 *J. Phys. Soc. Jpn.* **12** 570–586

[4] Kubo R 1966 *Rep. Prog. Phys.* **29** 255

[5] Dexter D L 1953 *J. Chem. Phys.* **21** 836–850

[6] Baumgartner B 1996 *J. Math. Phys.* **37** 5928–5938

[7] Ruelle D 2009 *Nonlinearity* **22** 855

[8] Pan L, Chen X, Chen Y and Zhai H 2020 *Nat. Phys.* **16** 1106–1111

[9] Hashemi A, Busch K, Christodoulides D N, Ozdemir S K and El-Ganainy R 2022 *Nat. Commun.* **13** 3281

[10] Sticlet D, Dóra B and Moca C u u u u P m c 2022 *Phys. Rev. Lett.* **128** 016802

[11] Sponselee K, Freystatzky L, Abeln B, Diem M, Hundt B, Kochanke A, Ponath T, Santra B, Mathey L, Sengstock K and Becker C 2018 *Quantum Sci. Technol.* **4** 014002

[12] Barontini G, Labouvie R, Stubenrauch F, Vogler A, Guarrera V and Ott H 2013 *Phys. Rev. Lett.* **110** 035302

[13] Ashida Y, Gong Z and Ueda M 2020 *Adv. Phys.* **69** 249–435

[14] Bergholtz E J, Budich J C and Kunst F K 2021 *Rev. Mod. Phys.* **93** 015005

[15] Lee T E 2016 *Phys. Rev. Lett.* **116** 133903

[16] Leykam D, Bliokh K Y, Huang C, Chong Y D and Nori F 2017 *Phys. Rev. Lett.* **118** 040401

[17] Shen H, Zhen B and Fu L 2018 *Phys. Rev. Lett.* **120** 146402

[18] Yao S and Wang Z 2018 *Phys. Rev. Lett.* **121** 086803

[19] Kunst F K, Edvardsson E, Budich J C and Bergholtz E J 2018 *Phys. Rev. Lett.* **121** 026808

[20] Gong Z, Ashida Y, Kawabata K, Takasan K, Higashikawa S and Ueda M 2018 *Phys. Rev. X* **8** 031079

[21] Kawabata K, Shiozaki K, Ueda M and Sato M 2019 *Phys. Rev. X* **9** 041015

[22] Lee J Y, Ahn J, Zhou H and Vishwanath A 2019 *Phys. Rev. Lett.* **123** 206404

[23] Wang C, Fu Z, Mao W, Qie J, Stone A D and Yang L 2023 *Adv. Opt. Photon.* **15** 442–523

[24] Li A, Wei H, Cotrufo M, Chen W, Mann S, Ni X, Xu B, Chen J, Wang J, Fan S, Qiu C W, Alù A and Chen L 2023 *Nat. Nanotechnol.* **18** 706–720

[25] Xiao L, Wang K, Qu D, Gao H, Lin Q, Bian Z, Zhan X and Xue P 2025 *Photonics Insights* **4** R09

[26] Lu P, Liu Y, Lao Q, Liu T, Rao X, Bian J, Wu H, Zhu F and Luo L 2025 *Commun. Phys.* **8** 91

[27] Li Y, Wu Y, Zhou Y, Zhang M, Zhao X, Yuan Y, Cheng X, Li Y, Qin X, Rong X, Lin Y and Du J 2025 *Quantum Front.* **4** 16

[28] Zhang Y, Carrasquilla J and Kim Y B 2025 *Nat. Commun.* **16** 3286

[29] Li J, Harter A K, Liu J, de Melo L, Joglekar Y N and Luo L 2019 *Nat. Commun.* **10** 855

[30] Zhang J, Li E Z, Wang Y J, Liu B, Zhang L H, Zhang Z Y, Shao S Y, Li Q, Chen H C, Ma Y, Han T Y, Wang Q F, Nan J D, Yin Y M, Zhu D Y, Guo G C, Ding D S and Shi B S 2025 *Nat. Commun.* **16** 3511

[31] Brody D C 2013 *J. Phys. A: Math. Theor.* **47** 035305

[32] Ma Y and Edelman A 1998 *Linear Algebra Appl.* **273** 45–63

[33] Heiss W D 2012 *J. Phys. A: Math. Theor.* **45** 444016

[34] Mandal I and Bergholtz E J 2021 *Phys. Rev. Lett.* **127** 186601

[35] Bai K, Li J Z, Liu T R, Fang L, Wan D and Xiao M 2023 *Phys. Rev. Lett.* **130** 266901

[36] Zhang Y X, Zhang Z T, Yang Z S, Wei X Z and Liang B L 2024 *Chin. Phys. B* **33** 060308

[37] Chen H, Zhou Y, Li X, Lou J, Luo S, Zhou H, Zhang X, Xu Z, Liu Y, Lv Z, Duan Y, Cheng H, Zhang H, Zhu Y, Li A, Ren J, Wang X, Zhang L, Zhang L and Chen Z 2026 *Chin. Phys. B* **35** 057105

[38] Bao L S, Ning J Y, Shi A Q, Peng P, Wang Z N, Peng C, Wen S C and Liu J J 2026 *Chin. Phys. B* **35** 010203

[39] Cao Y and Yan P 2019 *Phys. Rev. B* **99** 214415

[40] Zhang G Q and You J Q 2019 *Phys. Rev. B* **99** 054404

附录 A: FGR in Hermitian systems

For a Hermitian system, since the eigenstates $\{|\phi_n\rangle\}$ of the unperturbed Hamiltonian $\hat{H}_0$ form a complete set in the Hilbert space $\mathcal{H}$, for an arbitrary initial state $|\psi_0\rangle$, we can expand it as $|\psi_0\rangle = \sum_n a_n |\phi_n\rangle$. If we turn on a perturbation $\hat{V}(t)$ at time $t = 0$, then, at an arbitrary time t the state $|\psi_0\rangle$ evolves into:

$$|\psi(t)\rangle = \sum_n a_n(t) e^{-iE_n t} |\phi_n\rangle , \tag{A1}$$

which obeys the time-dependent Schrödinger equation:

$$\hat{H} |\psi(t)\rangle = (\hat{H}_0 + \hat{V}(t)) |\psi(t)\rangle = i\frac{\partial}{\partial t} |\psi(t)\rangle . \tag{A2}$$

Substitute Eq. (A1) into Eq. (A2) and we obtain:

$$[\hat{H}_0 + \hat{V}(t) - i\frac{\partial}{\partial t}] \sum_n a_n(t) e^{-iE_n t} |\phi_n\rangle = 0. \tag{A3}$$

Multiplying the above equation with $\langle\phi_f|$ from the left, and with the help of $\langle\phi_i|\phi_j\rangle = \delta_{i,j}$, we have:

$$i\hbar\frac{\mathrm{d}a_f(t)}{\mathrm{d}t} = \sum_n a_n(t)\left\langle\phi_f|\hat{V}(t)|\phi_n\right\rangle e^{i\omega_{fn}t}, \tag{A4}$$

where $\omega_{fn} \equiv E_f - E_n$.

Now, we assume that the initial state is one of the eigenstates of $\hat{H}_0$, say $|\phi_i\rangle$, i.e., $a_n(0) = \delta_{ni}$. If we confine our discussion to the case of weak perturbation, then, as a first-order approximation, we can substitute $a_n(t) = \delta_{ni}$ into (A4), which gives

$$i\frac{\mathrm{d}a_f(t)}{\mathrm{d}t} = \left\langle\phi_f|\hat{V}(t)|\phi_i\right\rangle e^{i\omega_{fi}t} \tag{A5}$$

The above equation integrates to

$$a_f(t) = -i\int_0^t \left\langle\phi_f|\hat{V}(\tau)|\phi_i\right\rangle e^{i\omega_{fi}\tau}d\tau. \tag{A6}$$

Now, we assume that the time-dependent disturbance $\hat{V}(t)$ is harmonic with the angular frequency ω, and has the form: $\hat{V}(t) = \hat{V}e^{-i\omega t}$, where $\hat{V}$ is time-independent.

Substituting the above expression into Eq.(A6), we arrive at

$$\begin{aligned} a_f(t) &= -i\left\langle\phi_f|\hat{V}|\phi_i\right\rangle\int_0^t e^{-i\omega\tau}e^{i\omega_{fi}\tau}d\tau, \\ &= -\left\langle\phi_f|\hat{V}|\phi_i\right\rangle\frac{e^{i(\omega_{fi}-\omega)t}-1}{\omega_{fi}-\omega}. \end{aligned} \tag{A7}$$

Further, with the help of the formula $\left|e^{i\theta}-1\right|^2 = 4\sin^2(\theta/2)$, the above equation can be written as:

$$P_{i\to f}(t) = |a_f(t)|^2 = \left|\langle\phi_f|\hat{V}|\phi_i\rangle\right|^2\frac{4\sin^2[(\omega_{fi}-\omega)t/2]}{(\omega_{fi}-\omega)^2}. \tag{A8}$$

In the limit $t\to 0$, the approximation $\sin^2[(\omega_{fi}-\omega)t/2] \approx [(\omega_{fi}-\omega)t/2]^2$ holds, which yields

$$P_{i\to f}(t\to 0) \approx \left|\langle\phi_f|\hat{V}|\phi_i\rangle\right|^2 t^2 \propto t^2, \tag{A9}$$

that is, the short-time transition probability is proportional to t^2.

On the other hand, according to one of the definitions of δ-function:

$$\delta(x) = \lim_{t\to\infty}\frac{1}{2\pi}\frac{\sin^2(tx/2)}{t(x/2)^2}, \tag{A10}$$

in the $t\to\infty$ limit, we have:

$$\begin{aligned} \frac{4\sin^2[(\omega_{fi}-\omega)t/2]}{(\omega_{fi}-\omega)^2} &= 2\pi t\delta(\omega_{fi}-\omega) \\ &= 2\pi t\delta(E_f - E_i - \omega), \end{aligned} \tag{A11}$$

Thus, Eq.(A8) can be written as:

$$P_{i\to f}(t\to\infty) = 2\pi t\left|\left\langle\phi_f|\hat{V}|\phi_i\right\rangle\right|^2\delta(E_f-E_i-\omega). \tag{A12}$$

The above expression is the transition probability in the long-time limit given by the conventional FGR.

附录 B: FGR in non-Hermitian systems without EPs

We now consider a non-Hermitian Hamiltonian $\hat{H}_0 \neq \hat{H}_0^\dagger$, whose right and left eigenstates satisfy the biorthogonality relation:

$$\begin{aligned} \hat{H}_0|\phi_n\rangle = E_n|\phi_n\rangle, \qquad \langle\chi_n|\hat{H}_0 = E_n\langle\chi_n|, \\ \langle\chi_n|\phi_m\rangle = \delta_{nm}, \end{aligned} \tag{B1}$$

and whose eigenvalues are generally complex:

$$E_n = \epsilon_n - i\gamma_n, \tag{B2}$$

where ϵ is the resonance energy, and γ is the dissipation rate.

In the absence of EPs, the results for the non-Hermitian system can be derived directly by following the procedure established for the Hermitian case. In the non-Hermitian setting, Eq. (A7) should accordingly be rewritten as:

$$\begin{aligned} a_f(t) &= -i\left\langle\chi_f|\hat{V}|\phi_i\right\rangle\int_0^t e^{-i\omega\tau}e^{i\omega_{fi}\tau}d\tau, \\ &= -\left\langle\chi_f|\hat{V}|\phi_i\right\rangle\frac{e^{i(\omega_{fi}-\omega)t}-1}{\omega_{fi}-\omega}. \end{aligned} \tag{B3}$$

where

$$\omega_{fi} = E_f - E_i = (\epsilon_f-\epsilon_i) - i(\gamma_f-\gamma_i) \equiv \omega_0 - i\Gamma, \tag{B4}$$

with ω_0 and Γ being real transition frequency and relative width parameter, respectively. The exact expression for the transition probability to a single final

state can be readily derived:

$$P_{i\to f}(t) = \left|\langle\chi_f|\hat{V}|\phi_i\rangle\right|^2 \frac{e^{2\Gamma t} + 1 - 2e^{\Gamma t}\cos(\Delta t)}{\Delta^2 + \Gamma^2} \quad \text{(B5)}$$

where $\Delta = \omega_0 - \omega$ is the Real detuning.

In the limit $t \to 0$, $e^{\Gamma t} \approx 1 + \Gamma t + \Gamma^2 t^2/2$, $e^{2\Gamma t} \approx 1 + 2\Gamma t + 2\Gamma^2 t^2$, $\cos(\Delta t) \approx 1 - \Delta^2 t^2/2$. Thus, we have:

$$e^{2\Gamma t} + 1 - 2e^{\Gamma t}\cos(\Delta t) \approx (\Delta^2 + \Gamma^2)t^2 \quad \text{(B6)}$$

where only the leading-order term in t is retained. Substituting this into Eq. (B8) gives:

$$P_{i\to f}(t \to 0) \approx \left|\langle\chi_f|\hat{V}|\phi_i\rangle\right|^2 t^2 \propto t^2, \quad \text{(B7)}$$

that is, as in the Hermitian case, for non-Hermitian systems without EPs, the transition probability is proportional to t^2 in the short-time limit.

We now turn to the long-time limit, which corresponds to the steady-state response of the system. In this regime, we consider the case $\Gamma < 0$. As $t \to \infty$, the transient term $e^{2\Gamma t}$ and $e^{\Gamma t}$ decays to zero, and we obtain:

$$\begin{aligned} P_{i\to f}(t \to \infty) &= \left|\langle\chi_f|\hat{V}|\phi_i\rangle\right|^2 \frac{1}{\Delta^2 + \Gamma^2} \\ &= \left|\langle\chi_f|\hat{V}|\phi_i\rangle\right|^2 \frac{1}{(\omega_0 - \omega)^2 + \Gamma^2}, \end{aligned} \quad \text{(B8)}$$

which is independent of time. Viewed as a function of the driving frequency ω, it exhibits an exact Lorentzian lineshape centered at the resonance frequency ω_0, with a full width at half maximum equal to 2Γ.